



# Dielectric-elastomer-based fabrication method for varifocal microlens array

LIHUI WANG,<sup>1,\*</sup> TOMOHIKO HAYAKAWA,<sup>1</sup> AND MASATOSHI ISHIKAWA<sup>1,2</sup>

<sup>1</sup>Department of Creative Informatics, University of Tokyo, 7-3-1 Hongo, Bunkyo-ku, Tokyo 113-8656, Japan

<sup>2</sup>Department of Information Physics and Computing, University of Tokyo, 7-3-1 Hongo, Bunkyo-ku, Tokyo 113-8656, Japan

\*wang\_lihui@ipc.i.u-tokyo.ac.jp

**Abstract:** We report on a method to fabricate a varifocal microlens array that employs a dielectric elastomer (DE) sandwiched between two electrodes as the lens material. The microlens array is patterned on the electrode plates, and when the electrodes are subjected to a controllable operating voltage, the DE material is “squeezed” by the Maxwell force to deform the lens array pattern, thus resulting in curvature deformation yielding a tunable lens profile. The tunable focal length performance ranges from 950 nm to infinity. When compared with liquid-filled lenses, solid-based varifocal lenses are more robust to thermal expansion, gravity, and vibrational motion. Our approach can be utilized in applications such as machine vision systems.

© 2017 Optical Society of America under the terms of the [OSA Open Access Publishing Agreement](#)

**OCIS codes:** (220.1080) Active or adaptive optics; (220.3620) Lens system design; (160.5470) Polymers; (230.2090) Electro-optical devices.

## References and links

1. J. E. Greivenkamp, *Field Guide to Geometrical Optics* (SPIE Publications, 2004).
2. H. Ren and S.-T. Wu, *Introduction to Adaptive Lenses* (John Wiley & Sons, 2012).
3. S. Sato, “Liquid-crystal lens-cells with variable focal length,” *Jpn. J. Appl. Phys.* **18**, 1679–1684 (1979).
4. M. Ye, B. Wang, M. Uchida, S. Yanase, S. Takahashi, and S. Sato, “Focus tuning by liquid crystal lens in imaging system,” *Appl. Opt.* **51**(31), 7630–7635 (2012).
5. G. Li, D. L. Mathine, P. Valley, P. Ayr s, J. N. Haddock, M. S. Giridhar, G. Williby, J. Schwiegerling, G. R. Meredith, B. Kippelen, S. Honkanen, and N. Peyghambarian, “Switchable electro-optic diffractive lens with high efficiency for ophthalmic applications,” *Proc. Natl. Acad. Sci. U.S.A.* **103**(16), 6100–6104 (2006).
6. Y. Lee, G. Tan, T. Zhan, Y. Weng, G. Liu, F. Gou, F. Peng, N. V. Tabiryan, S. Gauza, and S.-T. Wu, “Recent progress in Pancharatnam – Berry phase optical elements and the applications for virtual/augmented realities,” *Opt. Data Process. Storage* **3**, 79–88 (2017).
7. H. Oku, K. Hashimoto, and M. Ishikawa, “Variable-focus lens with 1-kHz bandwidth,” *Opt. Express* **12**(10), 2138–2149 (2004).
8. D.-Y. Zhang, V. Lien, Y. Berdichevsky, J. Choi, and Y.-H. Lo, “Fluidic adaptive lens with high focal length tunability,” *Appl. Phys. Lett.* **82**, 3171–3172 (2003).
9. N. Sugiura and S. Morita, “Variable-focus liquid-filled optical lens,” *Appl. Opt.* **32**(22), 4181–4186 (1993).
10. H. Ren, D. Fox, P. A. Anderson, B. Wu, and S.-T. Wu, “Tunable-focus liquid lens controlled using a servo motor,” *Opt. Express* **14**(18), 8031–8036 (2006).
11. H. Oku and M. Ishikawa, “High-speed liquid lens with 2 ms response and 80.3 nm root-mean-square wavefront error,” *Appl. Phys. Lett.* **94**, 221108 (2009).
12. L. Wang, H. Oku, and M. Ishikawa, “Variable-focus lens with 30 mm optical aperture based on liquid–membrane–liquid structure,” *Appl. Phys. Lett.* **102**, 131111 (2013).
13. L. Wang, H. Oku, and M. Ishikawa, “An improved low-optical-power variable focus lens with a large aperture,” *Opt. Express* **22**(16), 19448–19456 (2014).
14. B. Berge and J. Peseux, “Variable focal lens controlled by an external voltage: An application of electrowetting,” *Eur. Phys. J. E* **3**, 159–163 (2000).
15. S. Kuiper and B. H. W. Hendriks, “Variable-focus liquid lens for miniature cameras,” *Appl. Phys. Lett.* **85**, 1128–1130 (2004).
16. F. Mugele and J.-C. Baret, “Electrowetting: from basics to applications,” *J. Phys. Condens. Matter* **17**, R705–R774 (2005).
17. C.-C. Cheng, C. A. Chang, and J. A. Yeh, “Variable focus dielectric liquid droplet lens,” *Opt. Express* **14**(9), 4101–4106 (2006).
18. S. Xu, H. Ren, and S.-T. Wu, “Dielectrophoretically tunable optofluidic devices,” *J. Phys. D Appl. Phys.* **46**,

- 483001 (2013).
19. H. Zhang, H. Ren, S. Xu, and S. T. Wu, "Temperature effects on dielectric liquid lenses," *Opt. Express* **22**(2), 1930–1939 (2014).
  20. S. Xu, H. Ren, Y.-J. Lin, M. G. J. Moharam, S.-T. Wu, and N. Tabiryan, "Adaptive liquid lens actuated by photo-polymer," *Opt. Express* **17**(20), 17590–17595 (2009).
  21. S. Shian, R. M. Diebold, and D. R. Clarke, "Tunable lenses using transparent dielectric elastomer actuators," *Opt. Express* **21**(7), 8669–8676 (2013).
  22. L. Maffli, S. Rosset, M. Ghilardi, F. Carpi, and H. Shea, "Ultrafast all-polymer electrically tunable silicone lenses," *Adv. Funct. Mater.* **25**, 1656–1665 (2015).
  23. F. Carpi, G. Frediani, S. Turco, and D. De Rossi, "Bioinspired tunable lens with muscle-like electroactive elastomers," *Adv. Funct. Mater.* **21**, 4152–4158 (2011).
  24. A. S. Mondol, B. Vogel, and G. Bastian, "Large scale water lens for solar concentration," *Opt. Express* **23**(11), A692–A708 (2015).
  25. N. Hasan, A. Banerjee, H. Kim, and C. H. Mastrangelo, "Tunable-focus lens for adaptive eyeglasses," *Opt. Express* **25**(2), 1221–1233 (2017).
  26. F. Santiago, B. Bagwell, T. Martinez, S. Restaino, and S. Krishna, "Large aperture adaptive doublet polymer lens for imaging applications," *J. Opt. Soc. Am. A* **31**(8), 1842–1846 (2014).
  27. D. Koyama, R. Isago, and K. Nakamura, "Compact, high-speed variable-focus liquid lens using acoustic radiation force," *Opt. Express* **18**(24), 25158–25169 (2010).
  28. C. A. López, C.-C. Lee, and A. H. Hirs, "Electrochemically activated adaptive liquid lens," *Appl. Phys. Lett.* **87**, 134102 (2005).
  29. L. Miccio, A. Finizio, S. Grilli, V. Vespini, M. Paturzo, S. De Nicola, and P. Ferraro, "Tunable liquid microlens arrays in electrode-less configuration and their accurate characterization by interference microscopy," *Opt. Express* **17**(4), 2487–2499 (2009).
  30. A. O. Ashtiani and H. Jiang, "Thermally actuated tunable liquid microlens with sub-second response time," *Appl. Phys. Lett.* **103**, 111101 (2013).
  31. L. Dong, A. K. Agarwal, D. J. Beebe, and H. Jiang, "Adaptive liquid microlenses activated by stimuli-responsive hydrogels," *Nature* **442**(7102), 551–554 (2006).
  32. G. Beadie, M. L. Sandrock, M. J. Wiggins, R. S. Lepkowitz, J. S. Shirk, M. Ponting, Y. Yang, T. Kazmierczak, A. Hiltner, and E. Baer, "Tunable polymer lens," *Opt. Express* **16**(16), 11847–11857 (2008).
  33. J.-M. Choi, H.-M. Son, and Y.-J. Lee, "Biomimetic variable-focus lens system controlled by winding-type SMA actuator," *Opt. Express* **17**(10), 8152–8164 (2009).
  34. S. Yun, S. Park, B. Park, S. Nam, S. K. Park, and K. U. Kyung, "A thin film active-lens with translational control for dynamically programmable optical zoom," *Appl. Phys. Lett.* **107**, 081907 (2015).
  35. F. Carpi, G. Frediani, M. Nanni, and D. De Rossi, "Granularly coupled dielectric elastomer actuators," *IEEE/ASME Trans. Mechatron.* **16**, 16–23 (2011).
  36. Z. Suo, "Theory of dielectric elastomers," *Guti Lixue Xuebao* **23**, 549–578 (2010).
  37. C. Keplinger, J.-Y. Sun, C. C. Foo, P. Rothemund, G. M. Whitesides, and Z. Suo, "Stretchable, transparent, ionic conductors," *Science* **341**(6149), 984–987 (2013).
  38. L. Wang, H. Oku, and M. Ishikawa, "Paraxial ray solution for liquid-filled variable focus lenses," *Jpn. J. Appl. Phys.* **56**, 122501 (2017).
  39. E. Hecht, *Optics*, 4th ed. (Addison-Wesley, 2001).

## 1. Introduction

Lenses are essential components of many optical systems, and they are commonly used to transmit and/or bend light beams. Traditional lenses are constructed of solid materials such as glass and plastic. In order to realize zoom or focus functions, the conventional approach is to employ two or more lenses, which are mechanically moved over specific distances. Recent years have seen the prevalence of compact optical systems based on a variable-focus ("varifocal") lens, which is a single lens whose focal length can be changed dynamically.

The focal length of a lens is defined by the curvature of the refractive surface and the media on both sides, and a varifocal lens can be realized if at least one of these factors can be controlled [1,2]. In this regard, a liquid crystal (LC) lens forms a graded refractive index distribution via changing the orientations of the directors under the application of an inhomogeneous electric field, thereby controlling the focal length [3–6]. Another approach involves the manipulation of the physical deformation of the refractive surface of a liquid-filled lens. The mechanism of the focal length change is controlled by pumping a liquid into or out of a chamber. The classic operation mechanism utilizes a pumping system such as a syringe pump or a high-speed piezoelectric actuator to control the fluid pressure and the liquid volume so as to change the curvature of the lens profile [7–13]. The operation

mechanism is simple but an extra actuator is necessary. Along a different line of research, based on the principles of electrowetting phenomena, the curvature of an interface between an insulating liquid and a conducting liquid can be varied with the application of a controllable voltage, since the contacting angle is a function of the applied voltage [14–16]. Further, the interface angle of a high-dielectric liquid and a low-dielectric liquid can be controlled according to the dielectric force resulting from the application of an operating voltage [17,18]. Electrowetting devices and dielectrophoresis devices both use external voltage and can be driven silently, but they suffer from the problems of Joule heating and microbubble formation over long operating times [18]. Although two immiscible liquids with high transparency, equal density, and a large refractive index difference are considered to be ideal for this type of lens, it is difficult to prepare liquids with the same density at any temperature owing to thermal expansion [19]. In this regard, smart materials such as photopolymers [20] and dielectric elastomers (DEs) [21–23] have been employed to seal liquids in a chamber, and such systems when driven by blue-light irradiation or an operation voltage can reshape the lens profile, thereby resulting in change in the focal length. Various driving approaches based on fluidic pressure [24–26], acoustic radiation [27], electrochemistry [28], thermal effects [29,30], environmentally adaptive hydrogel [31], and other methods are currently available.

When compared with liquid-filled lenses, such solid-based varifocal lenses are more robust to thermal expansion, gravity, and vibrational motion, which makes the lenses ideal for practical applications. To the best of our knowledge, this area has attracted very little research. In a previous study, mechanical actuation by a rigid ring was designed to squeeze a transparent rubber in order to deform the lens profile [32]. Further, a soft polydimethylsiloxane (PDMS) lens was reportedly stretched by a surrounding muscle-like shape memory alloy (SMA) actuator [33]. Along similar lines, a combination lens system made of DE polymer and a PDMS lens with a translational movement along the vertical direction under application of various sinusoidal voltage signals has also been demonstrated [34].

Against this backdrop, in contrast to the abovementioned types of varifocal lenses, this research proposes a method to fabricate a varifocal microlens array based on a DE polymer, wherein the focal length of the system is changed by application of voltage. The proposed lens medium is a soft and controllable elastomer, as opposed to the approach of sealing optical liquid(s) within a chamber. Our proposed lens array exhibits a satisfactory varifocal performance.

## 2. Design principle and fabrication process

### 2.1 Design principle

A DE is a transparent smart material that can transform electrical energy into mechanical movement. When a voltage is applied to a DE, the electric field induces an effective compressive Maxwell stress across the elastomer. The resulting electrostatic pressure “squeezes” the DE material, thereby resulting in a decrease in its thickness and an increase in its area [35–37]. The DE is squeezed owing to electromechanical pressure  $P_{eq}$ , which can be expressed as

$$P_{eq} = \epsilon_0 \epsilon_r \frac{U^2}{d^2}, \quad (1)$$

where  $\epsilon_0$  represents the vacuum permittivity,  $\epsilon_r$  the dielectric constant of the DE material,  $d$  the thickness of the DE, and  $U$  the applied voltage. We assume that the refractive index does not change although the activated area is compressed and expands to the surrounding area.

When two electrode plates with a symmetric microlens array pattern are attached to the top and bottom of the DE elastomer and connected to a programmable voltage supply, a gradient voltage distribution is formed on the lens aperture zones. The zones with higher voltages, which are mainly on or close to the electrode plates, are subject to a greater electromechanical pressure; however, the zones within the apertures of the lens array are subject to lower voltage and consequently relatively less pressure. Since the DE material is soft, its squeezing leads to reshaping of the aperture zones. Each aperture cell on the lens array forms a lens profile. The focal length of the lens cell can thus be changed by controlling the applied voltage (Fig. 1).

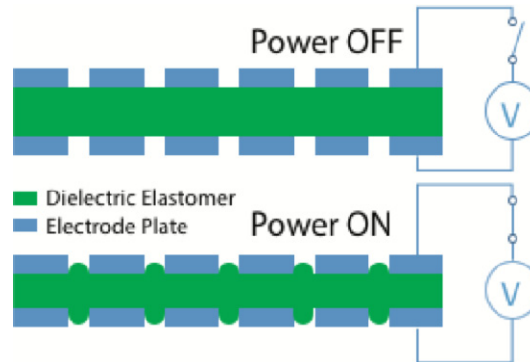


Fig. 1. Schematic of the varifocal microlens array based on dielectric elastomer (DE). The green color represents the DE material, and the blue color the electrode. Under the OFF state (no applied voltage), there is no deformation. In the ON state, the upper and lower electrodes squeeze the DE material via Maxwell stress, thereby resulting in curvature deformation of the “exposed” microlens array cells.

In the study, we first developed a model  $3 \times 3$  microlens array using the COMSOL simulation software. A 10-mm-diameter DE material was chosen, and a  $3 \times 3$  array with 1.5-mm-aperture cells was patterned on two (top and bottom) electrode plates, with each aperture being 1.5 mm in size. Polyacrylate was utilized as the DE material (dielectric constant  $\sim 4.7$ , density  $\sim 960 \text{ kg/m}^3$ , Young’s modulus  $\sim 220 \text{ KPa}$ , Poisson’s ratio  $\sim 4.9$ ). Figure 2 shows the voltage distribution obtained with the application of 5 kV between the top and bottom electrodes. While the electrode zone experienced the full voltage, the aperture was subjected to a relatively low voltage. The electromechanical pressure  $P_{eq}$ , which was calculated according to Eq. (1), was applied to the model. The deformation was confirmed by the simulation result, as shown in Fig. 2(C). Because the electromechanical pressure is a function of the voltage, the circular aperture portion of each cell (containing the “exposed DE”) will suffer a lower pressure and a smaller deformation, and would subsequently be reshaped as a lens profile.

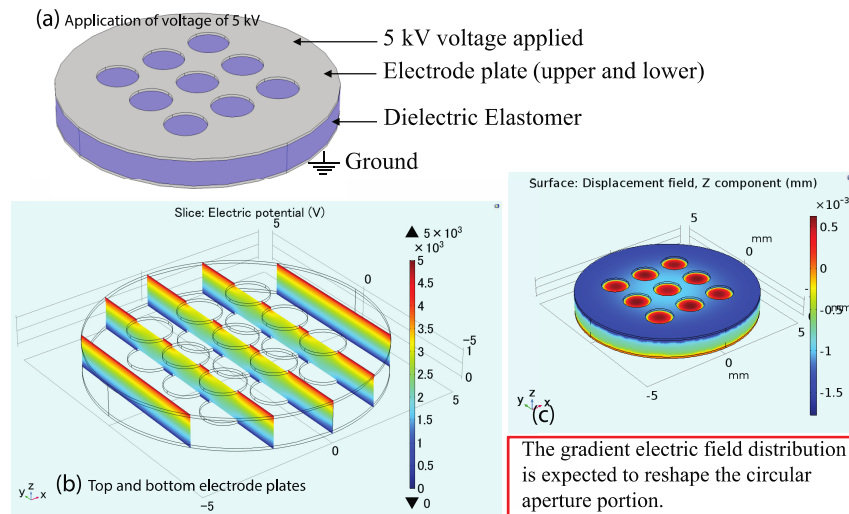


Fig. 2. Simulation result of voltage distribution of proposed dielectric elastomer (DE) upon application of 5 kV. Circularly shaped polyacrylate with a diameter of 10 mm was employed as the DE material. Two electrodes patterned with a  $3 \times 3$  array with 1.5-mm-aperture cells were affixed to the DE top and bottom surfaces. (a) Simulated model, (b) voltage distribution, and (c) displacement distribution.

## 2.2 Device fabrication

Based on our simulation results, we decided to develop an actual prototype of the proposed microlens array. We chose a soft DE material to fabricate our proposed varifocal microlens. The fabrication procedure is described below.

- First, we fabricated an insulating plastic frame with dimensions of  $40 \times 40$  mm and thickness of 1 mm, as shown in Fig. 3(a). An inner circular hole with a diameter of 30 mm was designed to fix the electrode plate.
- Stainless steel (SUS 303) was used as the plate material, shaped as a circular plate with a diameter of 30 mm. A  $9 \times 9$  aperture pattern was designed, with the aperture size of each cell being 1 mm in diameter. The plate was affixed to the insulated plastic frame, as shown in Fig. 3(b). We chose the electrode to be circular because we determined that electrical discharge occurred with square-shaped electrodes.
- In the third step, as shown in Fig. 3(c), we used a  $40 \times 40$  mm square-shaped, 1-mm-thick acrylic elastomer (3M, VHB 4910) as the DE material. The DE elastomer could be pasted on the electrode plates because VHB 4910 was originally designed as a double-sided adhesive tape.
- A second insulating plastic frame and electrode plate were fabricated and positioned on the top of the DE, as shown in Fig. 3(d).

The electrode plates were firmly affixed to the DE elastomer to ensure that they could squeeze the soft DE material via Maxwell forces upon application of the active voltage. Since the inner side of the aperture area (facing away from the electrode) is not subjected to high voltage, it “stores” the deformation and reshapes the profile of the DE material. The curvature of the DE material within the microlens aperture can be controlled according to the applied voltage on the electrode plates.

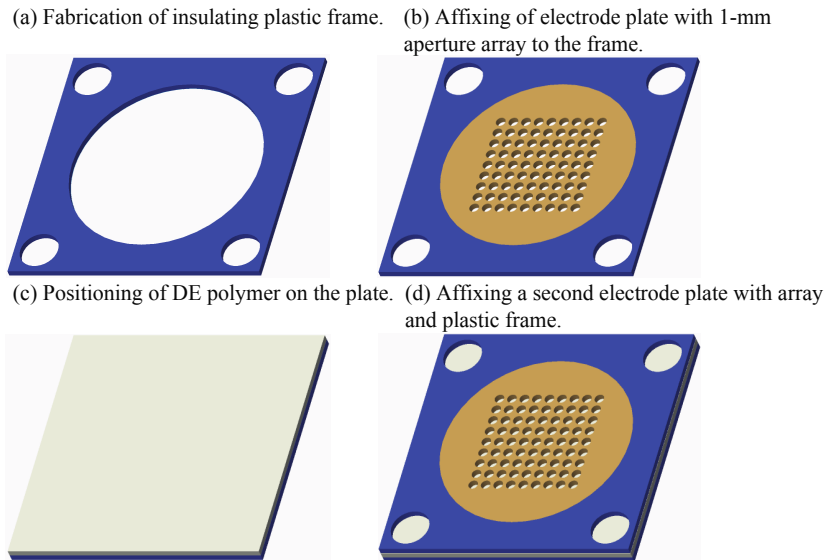


Fig. 3. Fabrication process of the dielectric elastomer (DE) microlens array device. (a) A  $40 \times 40$  mm square-shaped, 1-mm-thick insulating plastic plate with a 30-mm circular hole in the center is fabricated. (b) A circular stainless steel plate with 30-mm diameter forms the (bottom) electrode plate, and it is affixed to the plastic frame. A  $9 \times 9$  array is patterned on the plate, with each aperture size being set to 1 mm. (c) A  $40 \times 40$  mm, 1-mm-thickness acrylic elastomer (3M, VHB 4910) is employed as the DE material. The top and bottom electrode plates are pasted onto this DE material. (d) A second (top) electrode plate with an insulating plastic frame and electrode plate is affixed to the top surface of the DE material.

### 3. Experiment and discussion

#### 3.1 Experiment setup

To confirm the varifocal properties of our proposed microlens array system, we positioned our lens system between a camera and a target with depth information. Here, we recall that focal plane shifting is expected to occur when different voltages are applied to the lens system. Figure 4(a) illustrates our experimental setup. The target with depth information (Edmund Optics, DOF 5-15 Depth of Field Target) was positioned on one side of the test microlens array prototype, which is shown in Fig. 4(c). A camera (Edmund Optics, EO-1312C) was set on the opposite side, and a microlens kit (Edmund Optics, EO-39686 and EO-55359) was mounted on the camera for observation. In order to evaluate the varifocal performance of a single lens cell, a black occluder with an aperture that was slightly larger than the diameter of the microlens cell was positioned atop the test prototype, as shown in Fig. 4(b). A video clip of our experiment is linked with Fig. 4(d) ([Visualization 1](#)), which shows that the focal plane shifts from left to right of the target when the applied voltage is increased from zero to 5 kV. In our experiment, the applied voltage was increased in steps of 0.5 kV.

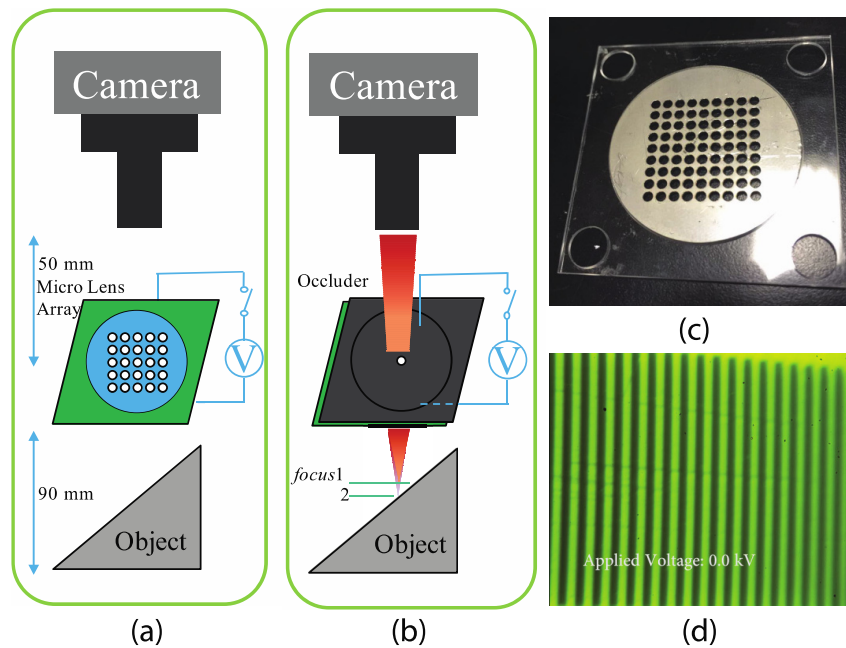


Fig. 4. (a) Experimental layout to determine varifocal lens performance. The microlens array is positioned in between a camera mounted with a lens kit and a target with depth information. (b) A black occluder with an aperture is positioned atop the lens prototype in order to evaluate the varifocal performance of a single lens cell. (c) Photograph of the microlens array prototype. (d) [Visualization 1](#) linked to a video clip showing the focus changing with the applied voltage.

### 3.2 Results and discussion

When no voltage was applied to the electrodes, there was no deformation of the DE material, and the image of the target with depth information was captured as shown in the upper left panel of Fig. 5. In contrast, the image corresponding to the application of 5 kV to the lens is shown in the lower left panel of Fig. 5.

Each of the photographs in the left panel shows a series of black and white lines (corresponding to the target). The photograph resolution was  $1024 \times 1280$  pixels. Considering the image as a matrix, the gradient of the change in the focal length was calculated as

$$\nabla F = \frac{\partial F}{\partial x} \hat{i} + \frac{\partial F}{\partial y} \hat{j}. \quad (2)$$

The above expression returns the  $x$  and  $y$  components of the 2D numerical gradient. Parameter  $F_x$  corresponds to  $\partial F / \partial x$ , the difference in focus along the  $x$  (horizontal)-direction, while  $F_y$  corresponds to  $\partial F / \partial y$ , the difference in focus along the  $y$  (vertical)-direction. The gradient was calculated along the red line shown in the left-panel images in Fig. 5. The gradient results were calculated with the use of MATLAB; the right panels of Fig. 5 show the corresponding gradient plots. A higher amplitude value indicates the area in focus.

We note from the figure that when the applied voltage is zero, the left portion of the image is in focus. Here, we also note that the horizontal axis of the gradient plot represents the pixel location along the red line, and thus, the top image confirms that the original focal point was in the near-field. When we gradually increased the applied voltage, the focal point dynamically moved from left to right (as reflected by the shift in the maximum amplitude from left to right in the plot), which meant that the focal point dynamically shifted from the left portion of the image to the right. Therefore, our results confirmed a change in the focal

length of the array with a change in the voltage applied to the DE material, thereby exhibiting agreement with our analysis in section 3.

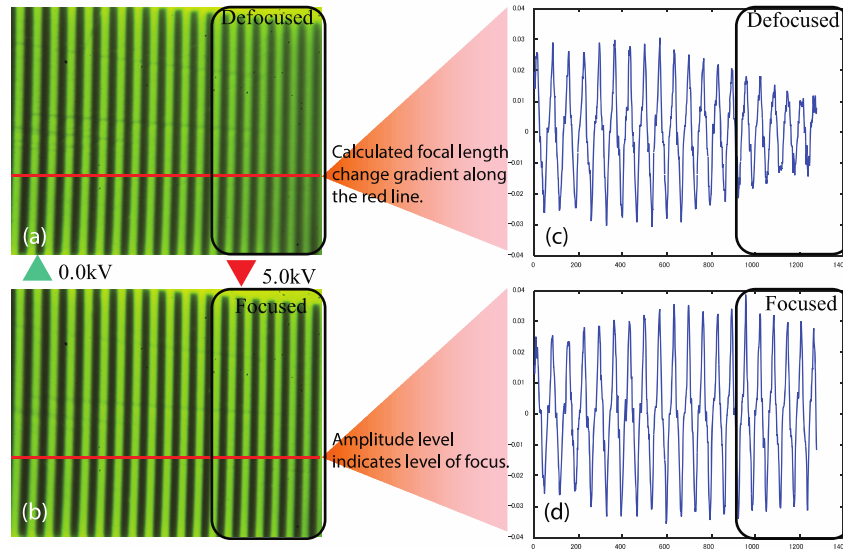


Fig. 5. Evaluation of varifocal performance of proposed microlens array. (a) Photograph of target with no applied voltage. The left portion of the image is in focus. (b) Photograph of target with application of 5 kV. The right portion of the image is in focus. To analyze the change in the focal plane, we calculated the focal change gradient using MATLAB. The gradient was calculated along the red line in (a) and (b). (c) and (d) Gradient plots corresponding to (a) and (b), respectively. The higher-amplitude region in the plot corresponds to the area in focus. The black box in (c) indicates that the image region corresponding to this box was defocused when the applied voltage was zero. In (d), the change in amplitude indicates the area being in focus with the application of 5 kV.

The distance between the camera lens system and the test lens was  $D = 50$  mm, with the initial (no applied voltage) combined focus of the camera and test lens  $f_1 = S_1 = 100$  mm [38,39]. When the operation voltage was zero, the focal length  $f_2$  of a single cell of the microlens array was infinity. The focal plane “moved” by  $S - S' = 2.5$  mm when 5 kV was applied to the DE and the focal length was  $f_2'$ . The values of parameters with prime symbols were updated after 5 kV voltage was applied. According to the focal plane movement and Eq. (3) below corresponding to the overall focal length, the focal length  $f_2'$  was calculated to be 950 mm; the corresponding schematic is shown in Fig. 6.

$$\frac{1}{f_2} = \frac{1}{S_2} - \frac{1}{S_1 - D}. \quad (3)$$

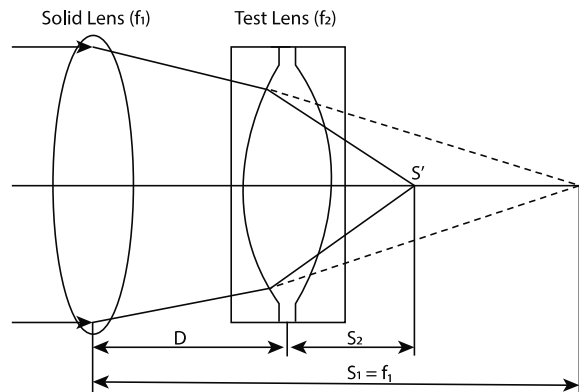


Fig. 6. Schematic depicting the change in the focal length of the test lens. The focal length of the test lens is  $f_2$ . With change in  $f_2$ , the combined focal plane shifts by a distance of  $S_2$ . The distance  $D$  between the camera lens and test lens is 50 mm, and with the initial combined focal length being  $f_1 = 100$  mm. When no voltage is applied to the DE, focal length  $f_2$  is infinity. When 5 kV is applied to the DE, the focal plane moves by  $S - S' = 2.5$  mm. The tunable range of the test lens is calculated as 950 mm to infinity.

In our experiment, the applied voltage was increased from zero to 5 kV in steps of 0.5 kV. When applying a higher voltage, electrical breakdowns occurred on the devices. The variation of the focal length  $f_2$  was calculated according to Eq. (3); the results are plotted in Fig. 7. The tunable focal length range of the microlens system was 950 mm to infinity. A monochrome camera (Mako-U130B, Allied Vision) was used, and a telecentric lens (TPC8-40D, Tokyo Parts Center) with coaxial illumination (IMH-250, Sigma Koki) was mounted. A 1951 US Air Force resolution test chart was employed as an imaging target and placed in front of the camera. The working distance from the lens to the target was 40 mm. The test microlens array prototype was inserted between them, 35 mm away from the camera lens. A black occluder with an aperture was positioned atop the test prototype so that one lens would be evaluated. An image was captured through the lens cell when the test lens was in the released state, as shown in the top right of Fig. 7. A resolution of 161.30  $lp/mm$  (Group 7, Element 3) was achieved.

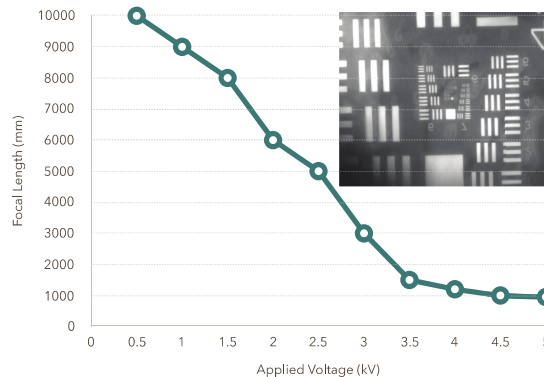


Fig. 7. Plot showing focal length changes at various voltages. In this experiment, the applied voltage was increased from zero to 5 kV in steps of 0.5 kV. The tunable focal length range of the microlens system was 950 mm to infinity. A 1951 USAF resolution test chart, shown in the top right, was captured through one of the microlens arrays.

#### 4. Conclusions

In this study, we proposed a method to fabricate a varifocal microlens array and demonstrated its varifocal performance. A dielectric elastomer (DE) was employed as the lens material, and it was sandwiched between two electrode plates. The microlens array was patterned on the electrode plates. When the electrode plates were subjected to a controlled voltage, the DE material was squeezed by Maxwell forces to deform the lens array pattern, thereby resulting in curvature deformation yielding a tunable lens profile. The tunable performance of the focal length was confirmed and analyzed by extracting the gradient profile of the change in focal length of a captured target photograph. The tunable range of the focal length was calculated to be 950 mm to infinity. When compared with liquid-filled lenses, solid-based varifocal lenses are more robust to thermal expansion, gravity, and vibrational motion. Our microlens array can be utilized in applications such as machine vision systems.

#### Funding

JSPS KAKENHI Grant-in-Aid for Young Scientists B 15K16035.

#### Acknowledgments

The authors would like to thank Dr. Dahai Mi in Keisoku Engineering System Co., Ltd. for helpful advice on COMSOL simulation, and Konica Minolta Inc. for partial financial support.